

Electronic Supplementary Information

New porous Co(II)-metal organic framework for high sorption selectivity and affinity for CO₂, and efficient catalytic oxidation of benzyl alcohols to benzaldehydes †

Yun-Long Wu,^{ab*} Rong-Rong Yang,^a Guo-Ping Yang,^b Yang-Tian Yan,^a Xiao-Lei Su,^a Xin-Hai He,^a Yan-Yan Song,^a Zheng-Sheng Ma^{b,II} and Yao-Yu Wang^b

^aSchool of Materials Science & Engineering, Xi'an Polytechnic University, Xi'an 710048, P. R. China

^bKey Laboratory of Synthetic and Natural Functional Molecule Chemistry of Ministry of Education, Shaanxi Key Laboratory of Physico-Inorganic Chemistry, College of Chemistry & Materials Science, and ^{II}School of Chemical Engineering, Northwest University, Xi'an 710127, P. R. China

*Corresponding author: 20180717@xpu.edu.cn.

Contents

I Tables

1. Selected bonds lengths [\AA] and angles [$^\circ$] for **I**.
2. The hydrogen bonds for **I**.
3. Comparison of selectivity for CO_2 at 298 K for **I'** and reported complexes.
4. Comparison of selectivity for CO_2 at 273 K for **I'** and reported complexes.
5. Optimization of the oxidation reactions.

II Figures

1. The chemical structure of the organic ligand H_4L .
2. The coordination models of carboxylate groups of the ligand.
3. The 1D porous networks contain dimethyl ammonium ions [Me_2NH_2^+] in **I**.
4. Topology analysis for **I**.
5. Pore structure of **I** from Materials Studio 6.0.
6. PXRD patterns of **I**, **I'** and sample after gas sorption and catalytic reaction.
7. FT-IR spectra of **I**, **I'** and sample after catalytic reaction.
8. TGA curves of **I** and **I'**.
9. N_2 adsorption isotherm for **I'** at 77 K.
10. CH_4 and CO_2 adsorption isotherms of **I'** at 273 K and 298 K with fitting by L-F model.
11. CO_2 adsorption isotherms for **I'** fitted by Virial model.
12. ^1H NMR spectra for the catalytic oxidation of benzyl alcohols into benzaldehydes.

I Tables

Table S1. Selected bonds lengths [Å] and angles [°] for **I**.

Complex I			
Co(1)-O(1)#1	2.024(2)	O(3)-Co(2)-N(1)#8	85.71(10)
Co(1)-O(1)	2.024(2)	O(4)-Co(2)-O(5)	84.49(9)
Co(1)-O(4)#2	2.155(2)	O(7)#7-Co(2)-O(2)#6	98.86(10)
Co(1)-O(4)#3	2.155(2)	O(7)#7-Co(2)-O(4)	94.38(10)
Co(1)-O(8)#4	2.063(2)	O(7)#7-Co(2)-O(5)	83.33(10)
Co(1)-O(8)#5	2.063(2)	O(7)#7-Co(2)-N(1)#8	88.21(10)
Co(2)-O(2)#6	2.141(2)	N(1)#8-Co(2)-O(2)#6	92.40(10)
Co(2)-O(3)	2.072(2)	N(1)#8-Co(2)-O(4)	171.31(9)
Co(2)-O(4)	2.160(2)	N(1)#8-Co(2)-O(5)	87.58(10)
Co(2)-O(5)	2.162(2)	C(22)-N(2)-C(23)	112.6(13)
Co(2)-O(7)#7	2.089(2)	C(22)-N(2)-C(24)	126.5(14)
Co(2)-N(1)#8	2.100(3)	C(24)-N(2)-C(23)	116.6(12)
N(2)-C(22)	1.354(15)	O(10)-C(22)-N(2)	111.6(15)
N(2)-C(23)	1.504(17)	O(10)-C(22)-H(22)	124.2
N(2)-C(24)	1.359(14)	N(2)-C(22)-H(22)	124.2
C(22)-H(22)	0.9500	N(2)-C(23)-H(23A)	109.5
C(23)-H(23A)	0.9800	N(2)-C(23)-H(23B)	109.5
C(23)-H(23B)	0.9800	N(2)-C(23)-H(23C)	109.5
C(23)-H(23C)	0.9800	H(24A)-C(24)-H(24B)	109.5
C(24)-H(24A)	0.9800	H(24A)-C(24)-H(24C)	109.5
C(24)-H(24B)	0.9800	H(24B)-C(24)-H(24C)	109.5
C(24)-H(24C)	0.9800	H(3A)-N(3)-H(3B)	107.8
N(3)-H(3A)	0.9100	C(25)-N(3)-H(3A)	109.1
N(3)-H(3B)	0.9100	C(25)-N(3)-H(3B)	109.1
N(3)-C(25)	1.364(10)	C(25)-N(3)-C(26)	112.6(9)
N(3)-C(26)	1.623(13)	C(26)-N(3)-H(3A)	109.1
C(25)-H(25A)	0.9800	C(26)-N(3)-H(3B)	109.1
C(25)-H(25B)	0.9800	H(23A)-C(23)-H(23B)	109.5
C(25)-H(25C)	0.9800	H(23A)-C(23)-H(23C)	109.5
C(26)-H(26A)	0.9800	H(23B)-C(23)-H(23C)	109.5
C(26)-H(26B)	0.9800	N(2)-C(22)-H(22)	124.2
C(26)-H(26C)	0.9800	N(2)-C(23)-H(23A)	109.5
O(1)#1-Co(1)-O(1)	180.0	N(2)-C(23)-H(23B)	109.5
O(1)-Co(1)-O(4)#2	84.89(10)	N(2)-C(23)-H(23C)	109.5
O(1)-Co(1)-O(4)#3	95.11(10)	H(23A)-C(23)-H(23B)	109.5
O(1)#1-Co(1)-O(4)#2	95.11(10)	H(23A)-C(23)-H(23C)	109.5

O(1)#1-Co(1)-O(4)#3	84.89(10)	H(23B)-C(23)-H(23C)	109.5
O(1)#1-Co(1)-O(8)#5	89.54(10)	N(2)-C(24)-H(24A)	109.5
O(1)#1-Co(1)-O(8)#4	90.46(10)	N(2)-C(24)-H(24B)	109.5
O(1)-Co(1)-O(8)#4	89.54(10)	N(2)-C(24)-H(24C)	109.5
O(1)-Co(1)-O(8)#5	90.46(10)	N(3)-C(25)-H(25A)	109.5
O(4)#2-Co(1)-O(4)#3	180.0	N(3)-C(25)-H(25B)	109.5
O(8)#4-Co(1)-O(4)#3	85.91(9)	N(3)-C(25)-H(25C)	109.5
O(8)#5-Co(1)-O(4)#2	85.91(9)	H(25A)-C(25)-H(25B)	109.5
O(8)#4-Co(1)-O(4)#2	94.09(9)	H(25A)-C(25)-H(25C)	109.5
O(8)#5-Co(1)-O(4)#3	94.09(9)	H(25B)-C(25)-H(25C)	109.5
O(8)#5-Co(1)-O(8)#4	180.00(12)	N(3)-C(26)-H(26A)	109.5
O(2)#6-Co(2)-O(4)	95.39(9)	N(3)-C(26)-H(26B)	109.5
O(2)#6-Co(2)-O(5)	177.81(10)	N(3)-C(26)-H(26C)	109.5
O(3)-Co(2)-O(2)#6	86.90(10)	H(26A)-C(26)-H(26B)	109.5
O(3)-Co(2)-O(4)	90.86(9)	H(26A)-C(26)-H(26C)	109.5
O(3)-Co(2)-O(5)	90.92(10)	H(26B)-C(26)-H(26C)	109.5
O(3)-Co(2)-O(7)#7	171.80(9)		

Symmetry Codes: #1-x+1, -y+2, -z+2; #2: -x+3/2, y+1/2, -z+3/2; #3: x-1/2, -y+3/2, z+1/2; #4: x, y, z+1; #5: -x+1, -y+2, -z+1; #6: -x+3/2, y-1/2, -z+3/2; #7: -x+3/2, y-1/2, -z+1/2; #8: -x+1, -y+1, -z+1.

Table S2. Hydrogen bonds for **1**.

D-H...A	d(D-H)	d(H...A)	d(D...A)	<(DHA)
O(4)-H(4A)...O(6)	0.815(19)	1.84(2)	2.621(3)	160(4)
O(4)-H(4B)...O(9)	0.826(19)	1.96(2)	2.747(4)	160(4)
C(22)-H(22)...O(9)	0.95	2.32	3.145(16)	144.3
C(24)-H(24A)...O(2)#2	0.98	2.53	3.314(14)	136.9
N(3)-H(3A)...O(6)	0.91	1.85	2.714(6)	158.5
N(3)-H(3B)...O(10)	0.91	1.70	2.578(14)	162.6

Symmetry Codes: -x+3/2, y+1/2, -z+3/2

Table S3. Comparison of selectivity for CO₂ over CH₄ at 298 K for **I'** and reported complexes.

Complexes	Selectivity	References
MIL-53(AI)	2.3	1
MOF-205-OBn	2.7	2
ZJNU-63	3.5	3
JLU-Liu18	4.5	4
MFM-130a	7.1	5
JLU-Liu46	9.8	6
(Me₂NH₂)₂[Co₃(L)₂(H₂O)₂]·2DMF	12.8	This work
[Ni(btzip)(H ₂ btzip)]·2DMF·2H ₂ O	13.9	7
{[PbZn(L) ₂]·DMA·H ₂ O} _n	16.2	8

Table S4. Comparison of selectivity for CO₂ over CH₄ at 273 K for **I'** and reported complexes.

Complexes	Selectivity	References
ZJNU-63	4.2	3
ZIF-95	4.3	9
ZIF-100	5.9	9
HKUST-1	7.1	10
MFM-130a	9.4	5
Cu ₂ (pbpta)	12	11
ZJU-16	38	12
{[PbZn(L) ₂]·DMA·H ₂ O} _n	41.3	9
(Me₂NH₂)₂[Co₃(L)₂(H₂O)₂]·2DMF	112	This work

References

- (1) Z. Xiang, X. Peng, X. Cheng, X. Li and D. Cao, *J. Phys. Chem. C.*, 2011, **115**, 19864–19871.
- (2) J. Sim, H. Yim, N. Ko, S. B. Choi, Y. Oh, H. J. Park, S. Park and J. Kim, *Dalton Trans.*, 2014, **43**, 18017–18024.
- (3) D. Bai, Y. Wang, M. He, X. Gao and Y. He, *Inorg. Chem. Front.*, 2018, **5**, 2227-2237.
- (4) W.-Q. Zhang, R.-D. Wang, Z.-B. Wu, Y.-F. Kang, Y.-P. Fan, X.-Q. Liang, P. Liu and Y.-Y. Wang, *Inorg. Chem.*, 2018, **57**, 1455-1463.
- (5) Y. Yan, M. Juríček, F.-X. Coudert, N. A. Vermeulen, S. Grunder, A. Dailly, W. Lewis, A. J. Blake, J. F. Stoddart and M. J. Schröder, *J. Am. Chem. Soc.*, 2016, **138**, 3371-3381.
- (6) B. Liu, S. Yao, X. Liu, X. Li, R. Krishna, G. Li, Q. Huo and Y. Liu, *ACS Appl. Mater Interfaces*, 2017, **9**, 32820-32828.
- (7) Y.-Z. Li, H.-H. Yang, H.-Y. Wang, L. Hou, Y.-Y. Wang and Z. Zhu, *Chem. Eur. J.*, 2018, **24**, 865–871.
- (8) J. Liu, G.-P. Yang, J. Jin, D. Wu, L.-F. Ma, Y.-Y. Wang, *Chem. Commun.*, 2020, **56**, 2395-2398.
- (9) B. Wang, A. P. Côté, H. Furukawa, M. O’Keeffe and O. M. Yaghi, *Nature.*, 2008, **453**, 207-212.
- (10) K.-S. Lin, A. K. Adhikari, C.-N. Ku, C.-L. Chiang and H. Kuo, *International Journal of Hydrogen Energy*, **2012**, **37**, 13865-13871.
- (11) G. Verma, S. Kumar, T. Pham, Z. Niu, L. Wojtas, J. A. Perman, Y.-S. Ch and S. Ma, *Cryst. Growth Des.*, 2017, **17**, 2711-2717.
- (12) K.-S. Lin, A. K. Adhikari, C.-N. Ku, C.-L. Chiang and H. Kuo, *International Journal of*

Table S5. Optimization of the oxidation reactions^a

Entry	Solvent	Cat (mol %)	Additive(mol %)	Time (h)	^b Yield (%)
1	toluene	I ⁺ (3 mol %)	proline (40%)	3h	21
2	2-propanol	I ⁺ (3 mol %)	proline (40%)	3h	NR
3	H ₂ O	I ⁺ (3 mol %)	proline (40%)	3h	<5
4	Acetic acid	I ⁺ (3 mol %)	proline (40%)	3h	<5
5	DMSO	I ⁺ (3 mol %)	proline (40%)	3h	37
6	CH ₃ CN	I ⁺ (3 mol %)	proline (40%)	3h	95
7	THF	I ⁺ (3 mol %)	proline (40%)	3h	NR
8	CH ₂ Cl ₂	I ⁺ (3 mol %)	proline (40%)	3h	Trace
9	DMF	I ⁺ (3 mol %)	proline (40%)	3h	47
10 ^c	CH ₃ CN	I ⁺ (3 mol %)	-	3h	41 ^c
11	CH ₃ CN	I ⁺ (3 mol %)	proline (5%)	3h	52
12	CH ₃ CN	I ⁺ (3 mol %)	proline (15%)	3h	68
13	CH ₃ CN	I ⁺ (3 mol %)	proline (30%)	3h	80
14	CH ₃ CN	I ⁺ (3 mol %)	proline (30%)	3h	89
15	CH ₃ CN	-	proline (40%)	3h	NR
16	CH ₃ CN	I ⁺ (1 mol %)	proline (40%)	3h	83
17	CH ₃ CN	I ⁺ (2 mol %)	proline (40%)	3h	89
18	CH ₃ CN	I ⁺ (5 mol %)	proline (40%)	3h	95
19	CH ₃ CN	Co(NO ₃) ₂ (3mol %)	proline (40%)	3h	Trace
20	CH ₃ CN	Co(OAc) ₂ (3mol %)	proline (40%)	3h	Trace

^aReaction conditions: **1a** (0.2 mmol), I⁺(3 mol %), solvent (2 mL), proline (x mol %), for 3 h.

^bIsolated yield; ^cThe by-product is benzoic acid, yield 13%, conversion 54%; no reaction (NR).

II Figures

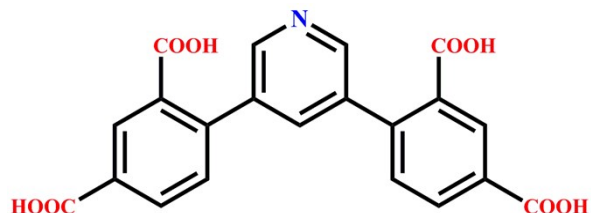


Fig. S1 The chemical structure of the v-shaped 3,5-di(2,4-dicarboxylphenyl)pyridine organic ligand H₄L.

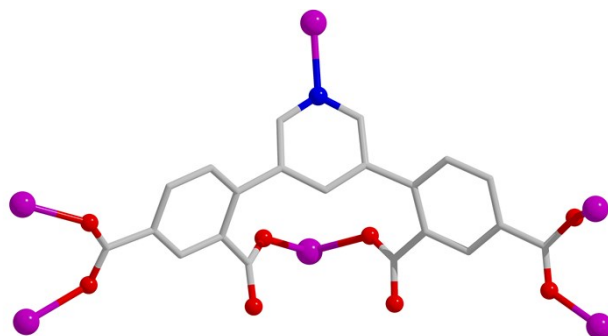


Fig. S2 The coordination model of carboxylic groups of the ligand in **I**: $\eta^2\mu_2\chi^2$ and $\eta^1\mu_1\chi^1$ (η -number of coordination bonds donated from the O atom of carboxylic groups from ligand; μ -number of metal centers bond the O atom of carboxylic groups from ligand; χ -number of coordination bonds).

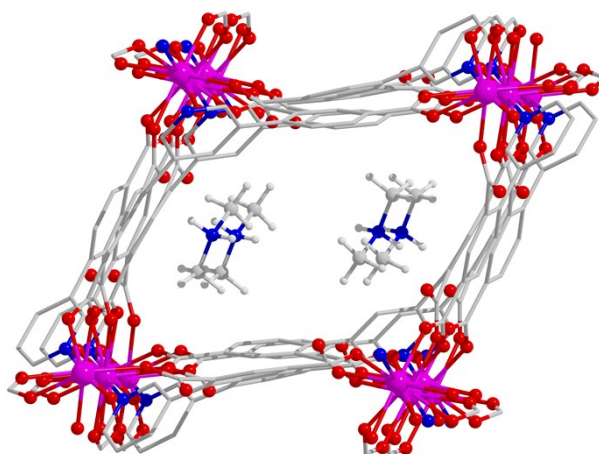
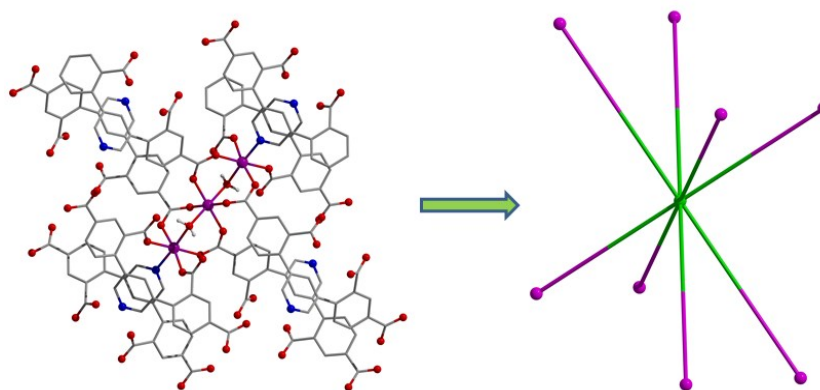
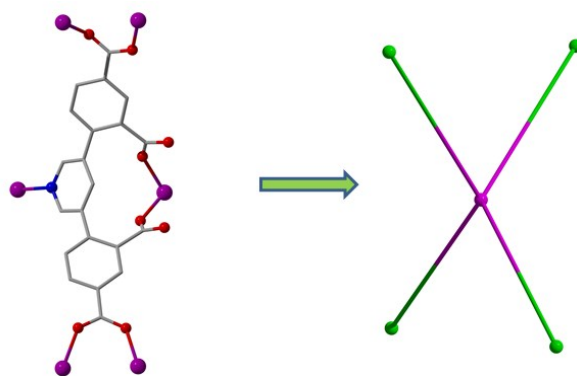


Fig.S3 The 1D porous network contains dimethyl ammonium ions $[\text{Me}_2\text{NH}_2^+]$ of **I**.



(a)



(b)

Fig. S4 Topology analysis for **I**: (a) simplified for the trinuclear SBUs $[\text{Co}_3(\text{COO})_4(\text{H}_2\text{O})_2\text{N}_2]$ as 8-connected nodes; (b) simplified for the organic ligand L^{4-} as 4-connected nodes.

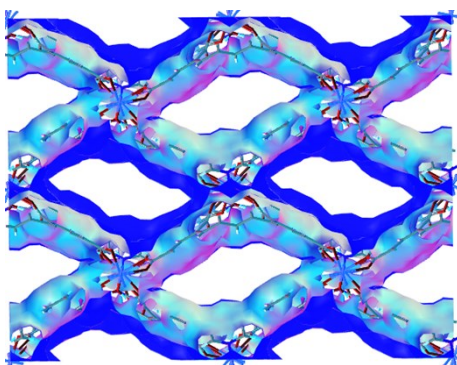


Fig. S5 Pore structure of **I** from Materials Studio 6.0.

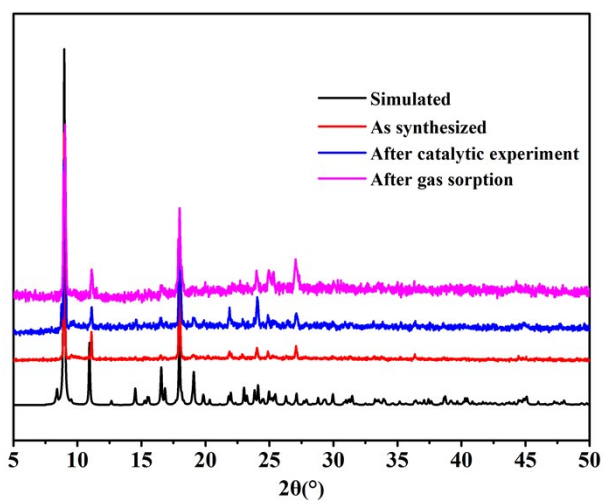


Fig. S6 PXRD patterns of **I** (simulated from crystal data; as synthesized; after catalytic and gas sorption experiments).

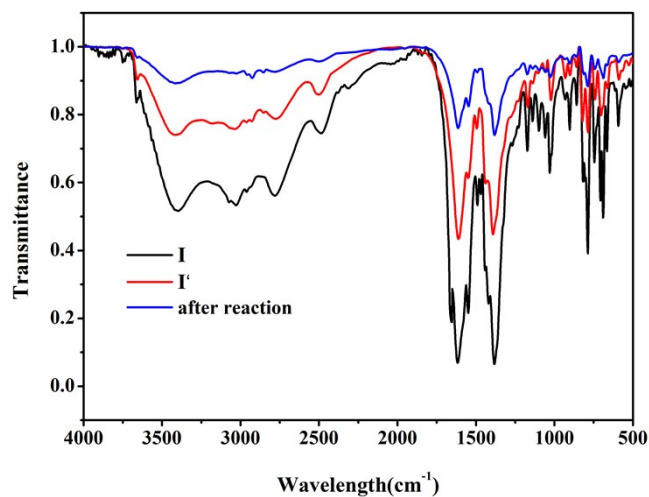


Fig. S7 The FT-IR spectra of complexes **I**, **I'** and the sample after catalytic reaction. The characteristic C=O vibration at 1663 cm^{-1} of DMF in **I** is absent in **I'**, indicating the complete removal of DMF.

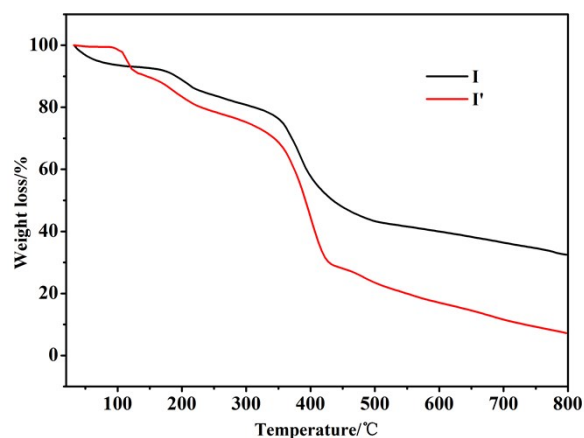


Fig. S8 TGA curves of the as-synthesized **I** and desolvated samples **I'**.

Gas adsorption test

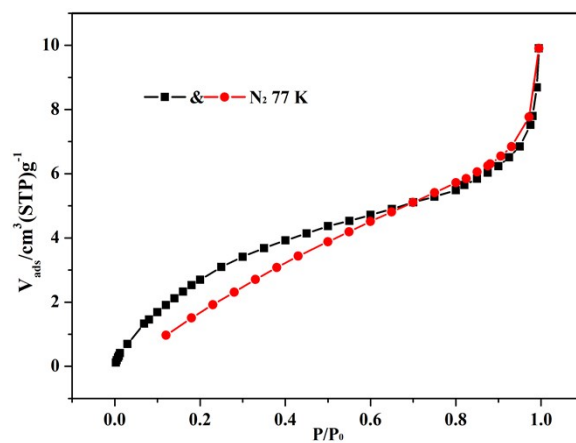


Fig. S9 N_2 adsorption isotherm for **I'** at 77 K.

IAST adsorption selectivity calculation:

The experimental isotherm data for pure CO₂ and CH₄ (measured at 273 and 298 K) were fitted using a Langmuir-Freundlich (L-F) model:

$$q = \frac{a * b * p^c}{1 + b * p^c}$$

Where q and p are adsorbed amounts and pressures of component i , respectively. The adsorption selectivities for binary mixtures of CO₂/CH₄ at 273 and 298 K, defined by

$$S_{ads} = (q_1 / q_2) / (p_1 / p_2)$$

Where q_i is the amount of i adsorbed and p_i is the partial pressure of i in the mixture.

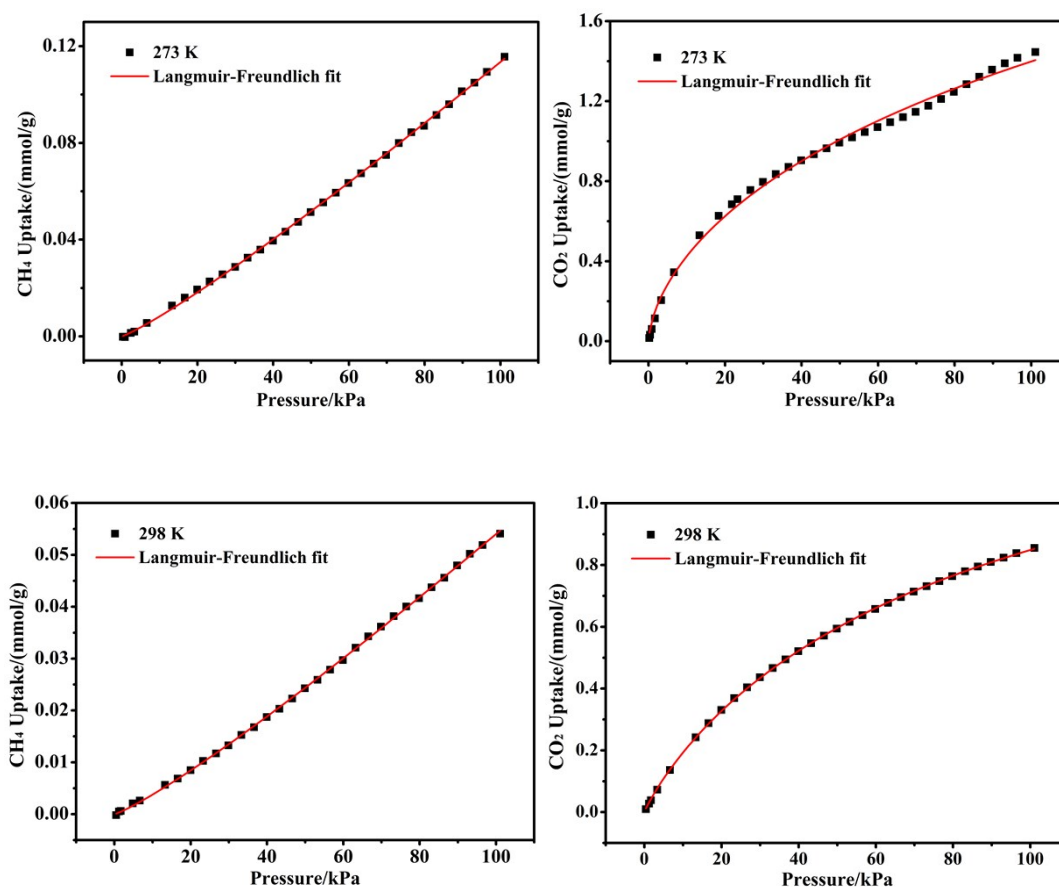


Fig. S10 CH₄ adsorption isotherms of **I'** at 273 K with fitting by L-F model: $a = 8.2443$, $b = 7.189 \times 10^{-5}$, $c = 1.14407$, $\chi^2 = 4.18 \times 10^{-7}$, $R^2 = 0.99969$; CO₂ adsorption isotherms of **I'** at 273 K with fitting by L-F model: $a = 5.01081$, $b = 0.02217$, $c = 0.62107$, $\chi^2 = 8.01 \times 10^{-4}$, $R^2 = 0.99559$; CH₄ adsorption isotherms of **I'** at 298 K with fitting by L-F model: $a = 2.93833$, $b = 8.84887 \times 10^{-5}$, $c = 1.16282$, $\chi^2 = 7.89072 \times 10^{-8}$, $R^2 = 0.99973$; CO₂ adsorption isotherms of **I'** at 298 K with fitting by L-F model: $a = 1.64397$, $b = 0.01654$, $c = 0.90479$, $\chi^2 = 6.5063 \times 10^{-6}$, $R^2 = 0.99991$.

Calculation of sorption heat for CO₂ uptake using Virial 2 model

$$\ln P = \ln N + 1/T \sum_{i=0}^m aiN^i + \sum_{i=0}^n biN^i Q_{st} = -R \sum_{i=0}^m aiN^i$$

The above equation was applied to fit the combined CO₂ isotherm data for **I'** at 273 and 298 K, where P is the pressure, N is the adsorbed amount, T is the temperature, ai and bi are virial coefficients, and m and n are the number of coefficients used to describe the isotherms. Q_{st} is the coverage-dependent enthalpy of adsorption and R is the universal gas constant.

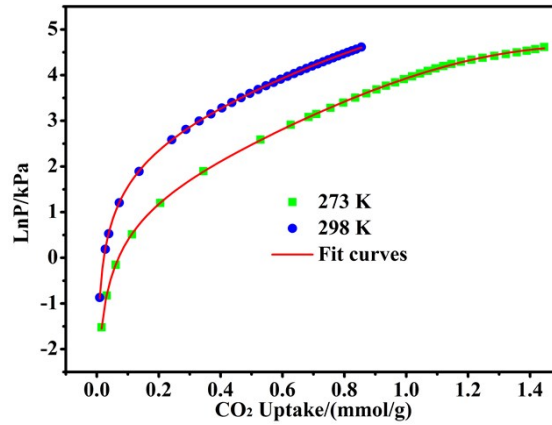
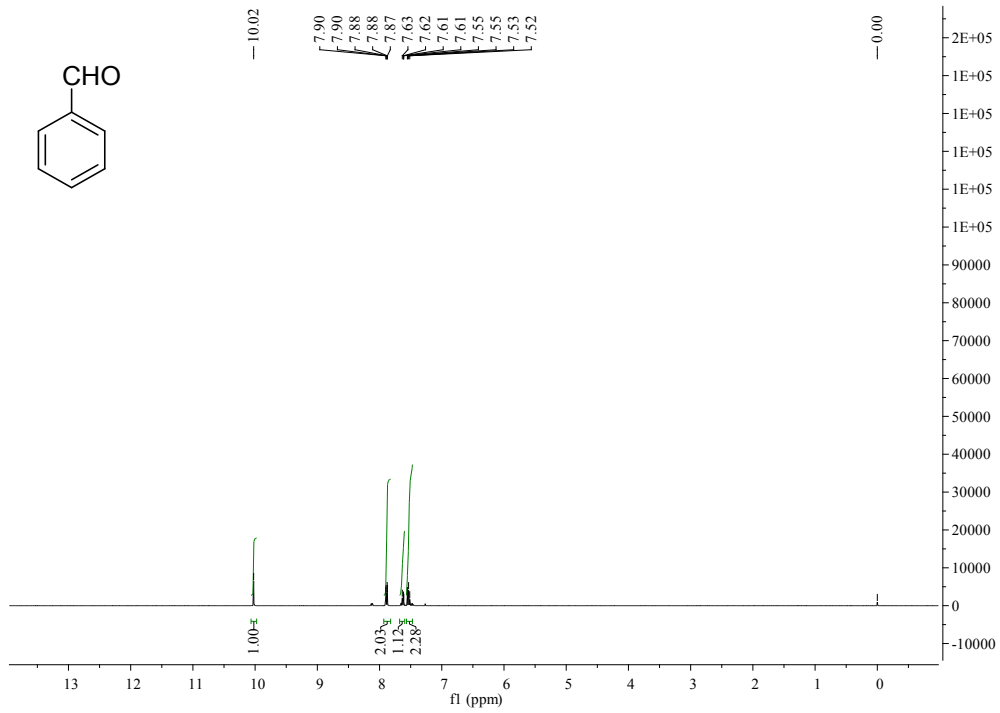
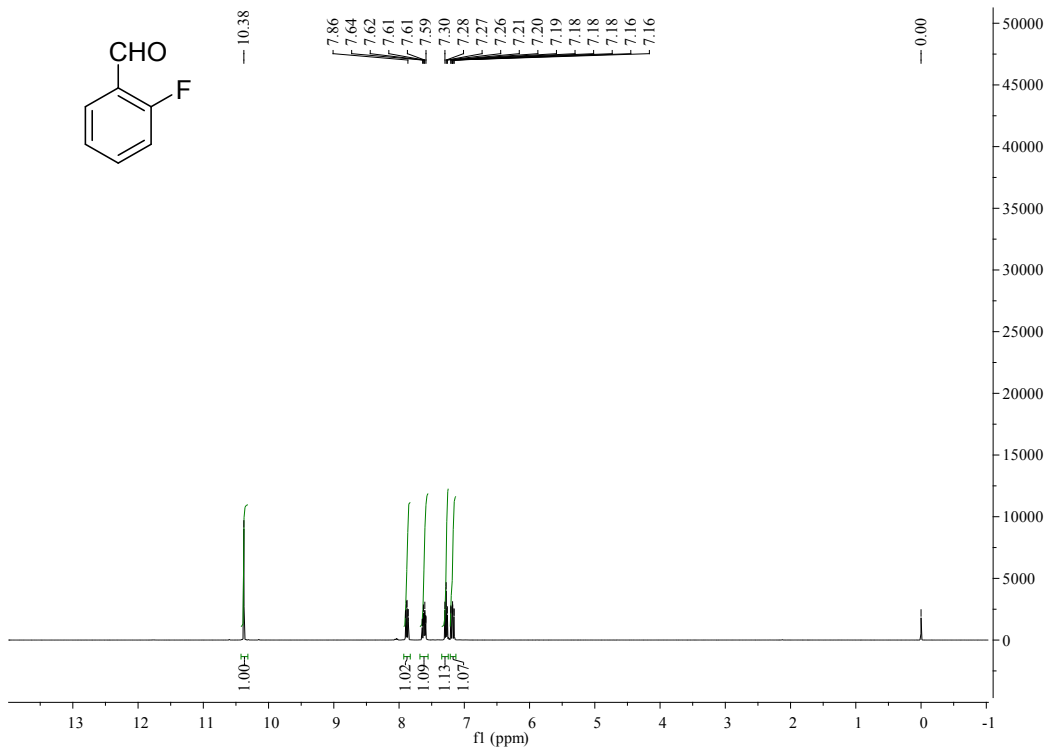


Fig. S11 CO₂ adsorption isotherms for **I'** fitted by Virial model. Fitting results: $a_0 = -3791.44891$; $a_1 = -295.74484$; $a_2 = 886.17577$; $a_3 = 278.32264$; $a_4 = -345.5531$; $a_5 = 81.96688$; $b_0 = 16.49525$; $b_1 = 1.83753$; $b_2 = -2.73299$; $\chi^2 = 1.26359 \times 10^{-4}$; $R^2 = 0.99994$.

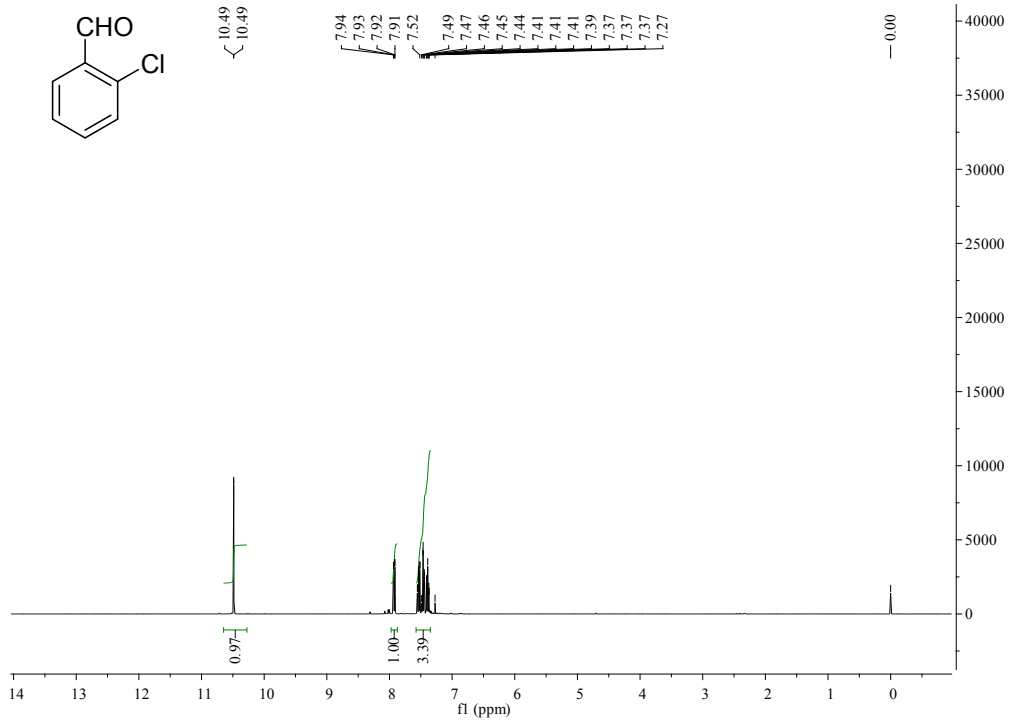
¹H NMR spectra of compound **2a**



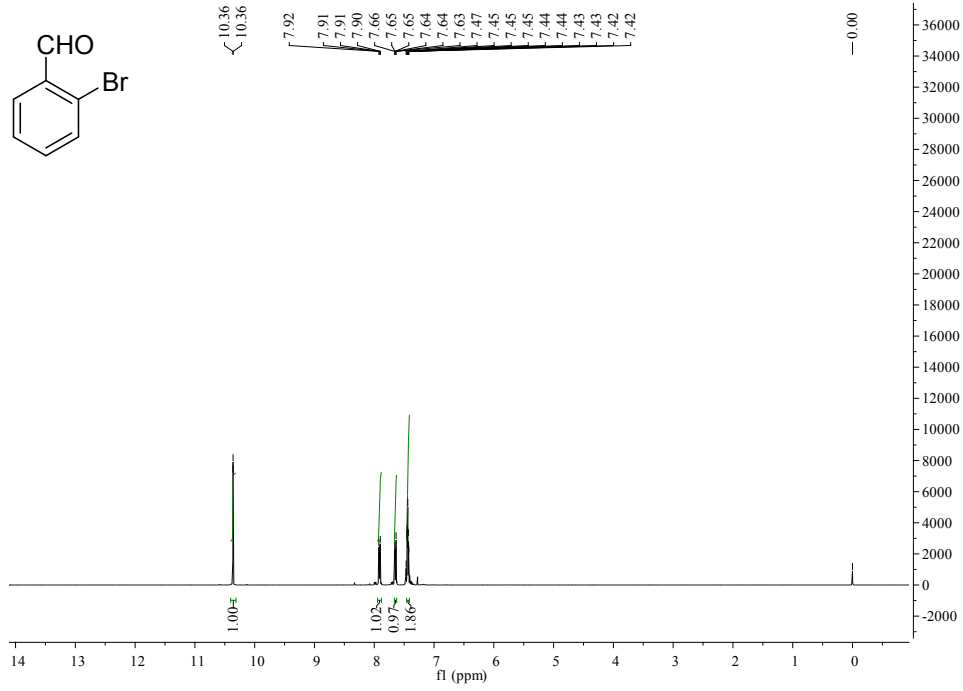
¹H NMR spectra of compound **2b**



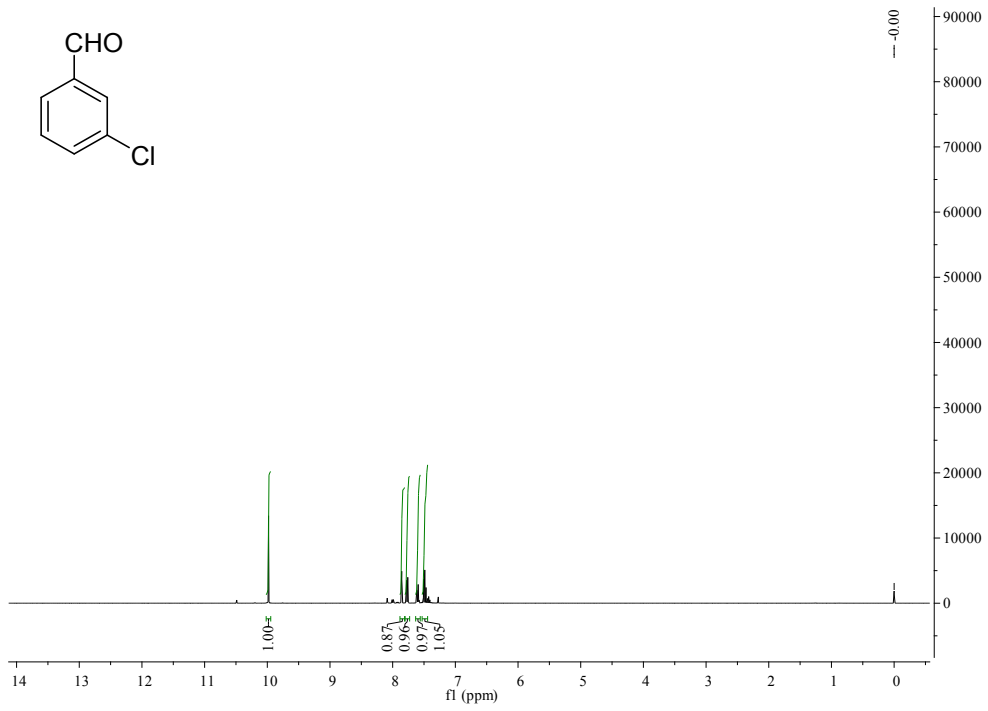
¹H NMR spectra of compound 2c



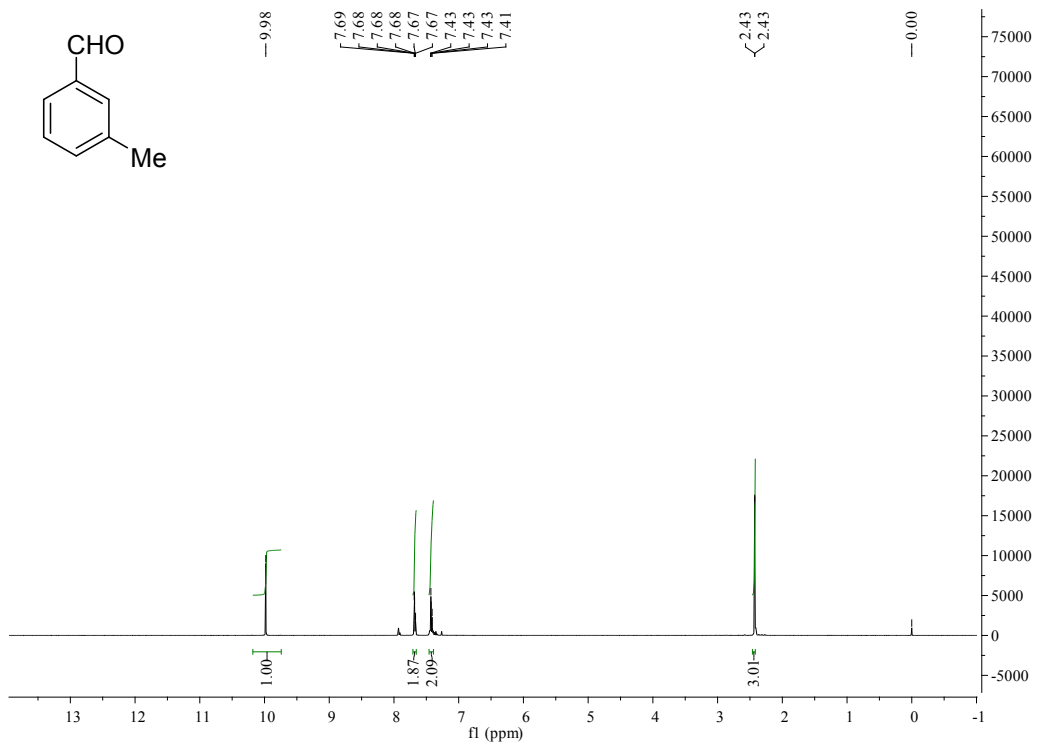
¹H NMR spectra of compound 2d



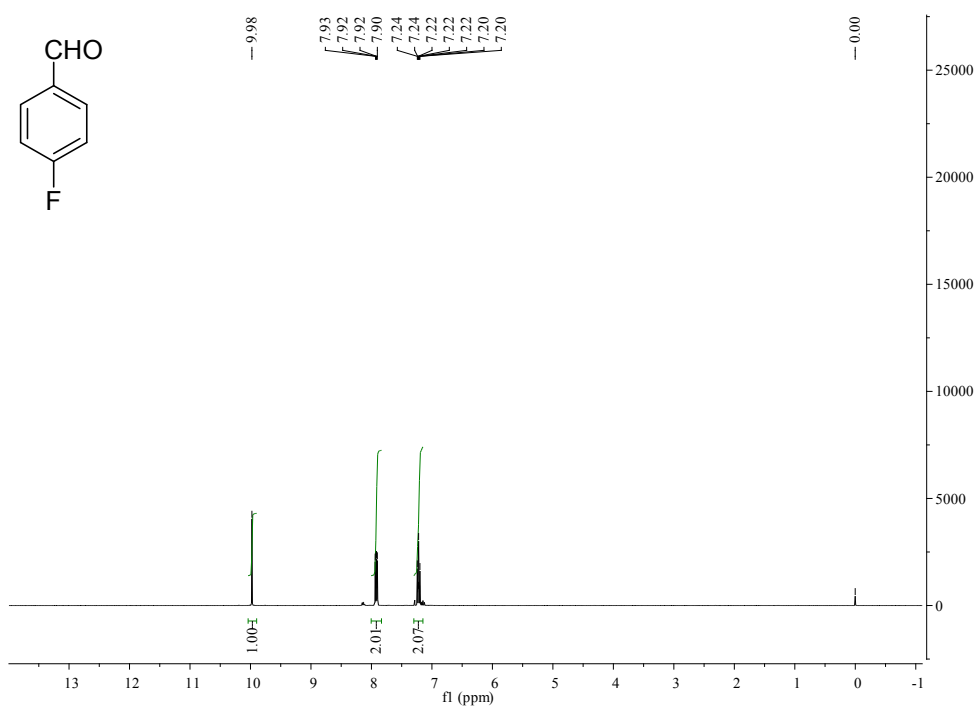
¹H NMR spectra of compound **2e**



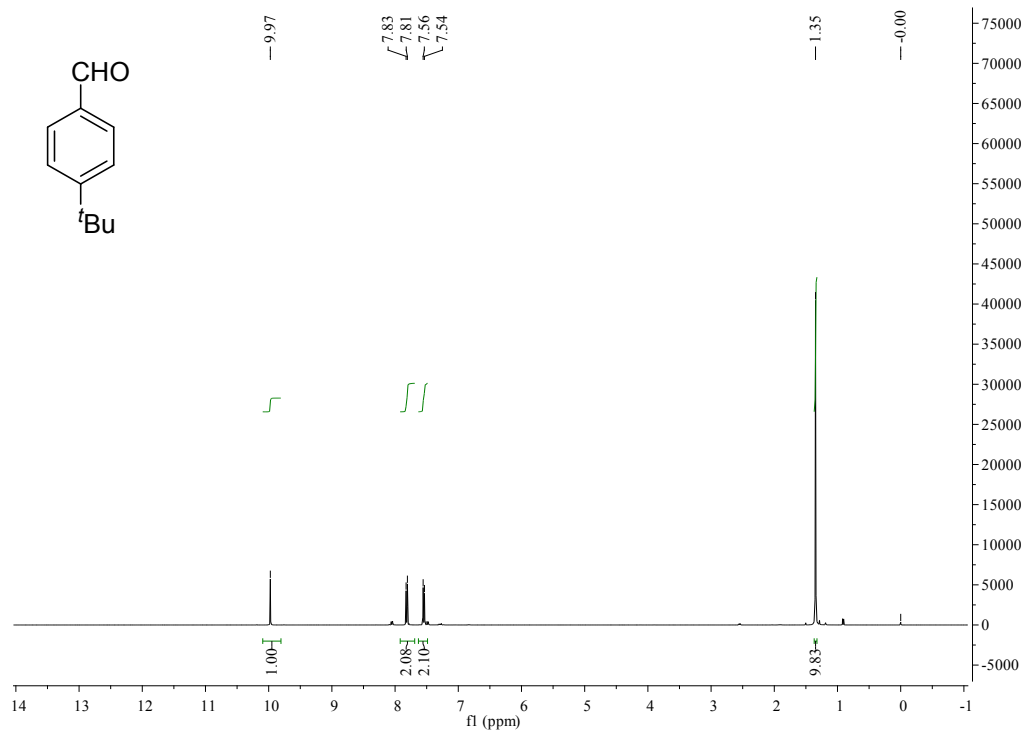
¹H NMR spectra of compound **2f**



¹H NMR spectra of compound **2g**



¹H NMR spectra of compound **2h**



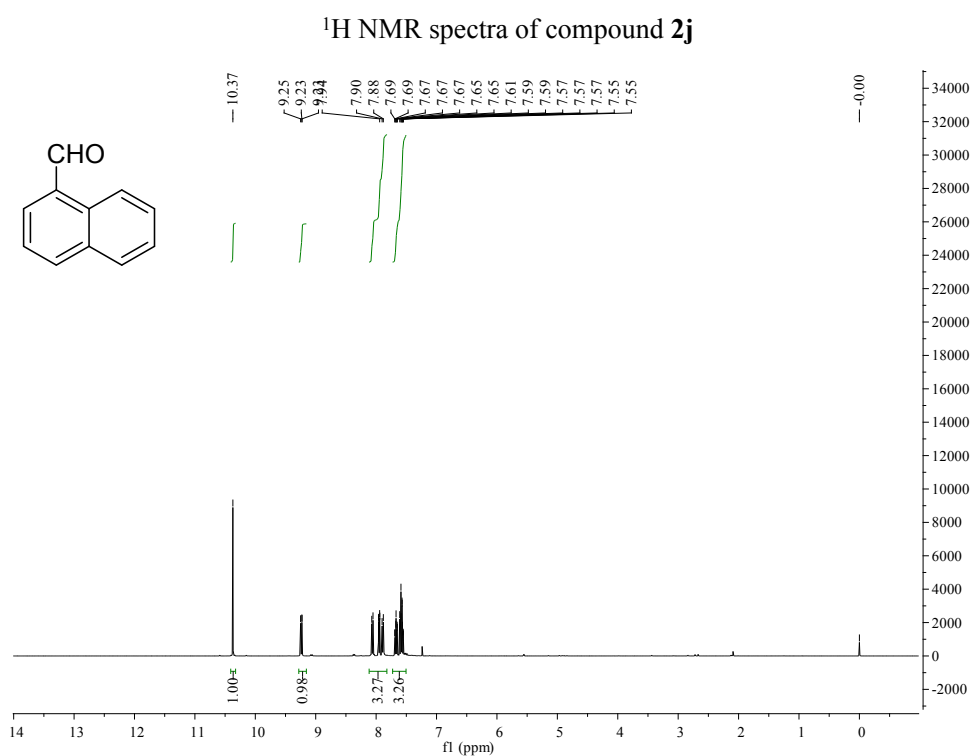
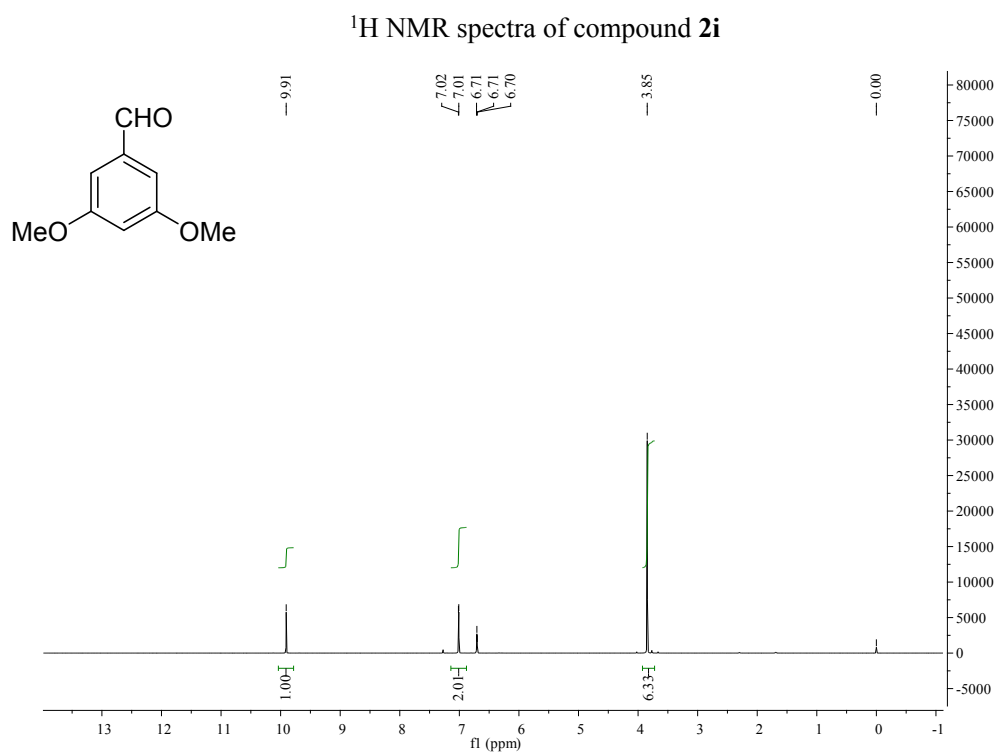


Fig. S12 ¹H NMR spectra for the catalytic oxidation of benzyl alcohols into benzaldehydes (¹H NMR).